

CONTROLLED MULTICHANNEL DISCHARGERS WITH WATER INSULATION

V. V. Balalaev, N. K. Kapishnikov,
V. M. Muratov, and V. Ya. Ushakov

UDC 621.374.2

Controlled gas-filled or liquid dischargers [1-3] are used as switches in the majority of existing nanosecond accelerators and x-ray generators. The use of gas dischargers is convenient at voltages up to 2-3 MV, while liquid dischargers can be used at practically any voltages [1].

One of the most promising liquid dischargers being used in nanosecond accelerators [4, 5] is the three-electrode discharger controlled by an additional gas-filled switch. However, the lack of sufficiently complete data on the characteristics and constructional principles of such dischargers has restricted their use, while the low stability of their operation compared with gas-filled switches has stimulated a further search for optimum modes of operation, constructions, and methods of triggering the dischargers with liquid insulation.

In this investigation we used two different methods of triggering controlled dischargers, which switch a coaxial storage line with a wave impedance $Z_w = 4.6 \Omega$. The insulation of the line is water with a volume resistivity $\rho = 2 \cdot 10^6 \Omega \cdot \text{cm}$ (Fig. 1). The double electrical length of the shaping and transmission lines are 40 nsec and 25 nsec, respectively [6]; the diameter of the inner cylinder (the body of the store) is 0.4 m. The shaping line is charged from a Marx generator up to an amplitude of 0.6-1.0 MV in a time of $\approx 0.75 \mu\text{sec}$. In the experiments we recorded the following: the charge voltage and the delay time of the operation of the dischargers with a resistive divider D_1 and a capacity divider D_3 , the discharge current from the shunt ($R_{sh} = 0.022 \Omega$), built into a cut in the outer cylinder of the transmission line, and also the optical phenomena in the discharge gap using two ZIM-2 electron-optical shutters (exposure - 10 nsec; time between frames - 40 nsec) while simultaneously photographing the discharge channels with a static camera. The divider D_1 is made of Nichrome wire, wound bifilarly on a PVC tube 0.16 m in diameter and 1.6 m long ($R_1 = 18 \text{ k}\Omega$, $R_2 = 20.5 \Omega$). The divider D_3 consists of a low-voltage cylindrical capacitor C_2 , embedded in the body of the store, and a high-voltage capacitor C_1 formed by the inner electrode of C_2 and the inner cylinder of the store. The calculated values of C_1 and C_2 are 10 pF and 500 pF, respectively, and the time constant of the divider is $< 5 \text{ nsec}$.

We investigated the following fundamental characteristics of the discharger: 1) the delay time of the operation of the discharger t_d measured from the instant when the initiating agent acts until breakdown of the main gap; 2) the operating stability σ_0 , viz., the mean-square deviation of the value of t_d ; 3) the switching time t_s or the rise time of the current pulse, determined by a standard method; 4) the effective value of the switched current I at the level of the calculated pulse lengths.

Three-Electrode Discharger. The main elements of the switch, which are component elements of the shaping and transmission lines (see Fig. 1), are made of stainless steel in the form of rings with an external diameter of 12 cm and thickness 3 cm. The controlling electrode, which is a disk with a sharp edge of diameter of 10 cm and thickness 0.4 cm, is made in the shape of a circular knife of Kh18N10T stainless steel, placed close to the transmission line and attached to a caprolon insulator (the body of the protective resistance). The ratio of the gaps was kept constant at 7:1 [1] with an overall interelectrode spacing $d = 5 \text{ cm}$. The control electrode was connected to the gas-filled discharger P_2 through a liquid protective resistance ($\sim 1 \text{ k}\Omega$). The discharger P_2 was triggered from a trigger-pulse generator 0.55 μsec after the start of the charging of the shaping line, i.e., and the instant when the amplitude of the line charging voltage reaches $0.8U_{\text{max}}$. The amplitude of the trigger signal U_t is 35 kV and the rise time is 3 nsec. The trigger time was chosen on the basis of experimental data on the rate of development of the discharge.

Figure 2 shows t_d and σ_0 as a function of the amplitude of the working voltage. The time t_d was found by measuring the signals from D_3 and D_2 on an oscilloscope. The minimum values $t_d = 200 \text{ nsec}$ and $\sigma_0 = 15 \text{ nsec}$

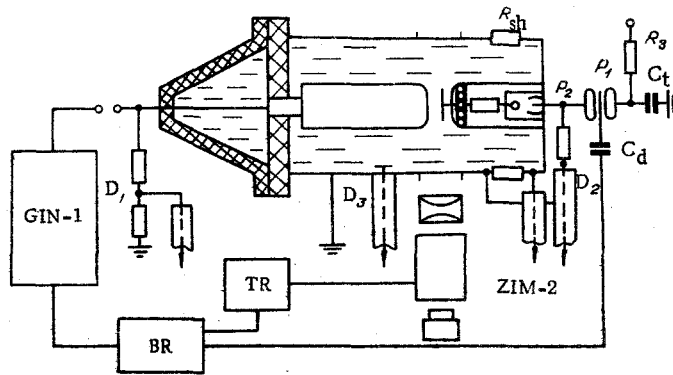


Fig. 1

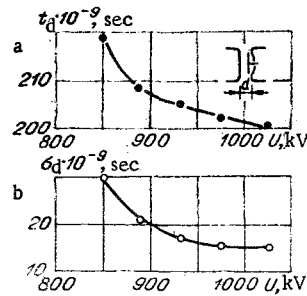


Fig. 2

were obtained for $U = 1000$ kV ($0.9U_t$ initiated from the anode). A reduction in the working voltage by 15% leads to an increase in σ_0 by a factor of two. For voltages close to the self-breakdown voltage ($0.95-1.0$) U_t , σ_0 increases by 10-20% due to spontaneous triggering. The voltage range over which, as a result of controlled initiation, multichannel switching (a discharge with respect to two or more channels) occurs with a probability of 0.9 is $(0.85-0.95)U_t$. The fact that switching occurred over several channels follows from the frame photographs (Figs. 3a and b) and the static photographs of the discharge (Fig. 3c), and also from a comparison of the current oscillograms characteristic for single and multichannel switching (Figs. 4a and b, respectively; $U = 860$ kV, calibration frequency 10^8 Hz). The oscillations on the leading edge of the pulse are due to transients in the line.

With the aid of the frame photographs, we followed the development of the discharge channels at different instants of time. For example, for $U = 880$ kV, 50 nsec after triggering of the gas discharger P_2 numerous channels (20-30) are formed in the region of the sharp edge of the control electrode, which propagate towards the potential electrode at an average speed of $(2-4) \cdot 10^6$ cm/sec (Fig. 3a). Some 100 nsec after the discharger P_2 triggers a preferred development of 3-6 channels is observed (Fig. 3b), the velocity of which over the section $(0.2-0.3)d$ exceeds the speed of development of the majority of channels by approximately an order of magnitude. As they penetrate further (the $(0.8-1)d$ section) the mean speed increases to $(6-8) \cdot 10^7$ cm/sec. After breakdown of the first gap the total voltage is applied to the second gap, which ensures short firing times and the development of discharge channels in the second gap. Irrespective of the dependence on the number of channels in the first gap, switching occurs in the second gap over 4-6 channels. In the case when a gap is simultaneously covered by several channels the brightness and diameter of the illumination of the discharge channels are approximately the same; then the reduction in the current amplitude compared with the calculated value does not exceed 20-25%, whereas for switching in a single channel it may be as high as 30-40%.

Damage of the electrode by erosion and shock waves produced by the spark considerably increases the spread in the firing of the discharge, and reduces the probability of switching in several channels only after $\approx 800-1000$ "shots." After ≈ 1000 operations of the discharger for a charging voltage of $(0.85-0.95)U_t$, the mean-square deviation σ_0 increases by 30-40%, while the probability of simultaneous switching over 2-3 channels becomes 50%. The operational reserve of the discharges under multichannel conditions can be increased by further increasing the number of effective channels and the length of the working edge of the control electrode.

Trigatron Dischargers. The high triggering stability of a water trigatron can be achieved by initiating a discharge with an "intensified field" in the region of the anode, when the main gap breaks down earlier than the "keep-alive" electrode, and the triggering pulse has a nanosecond rise time [7].

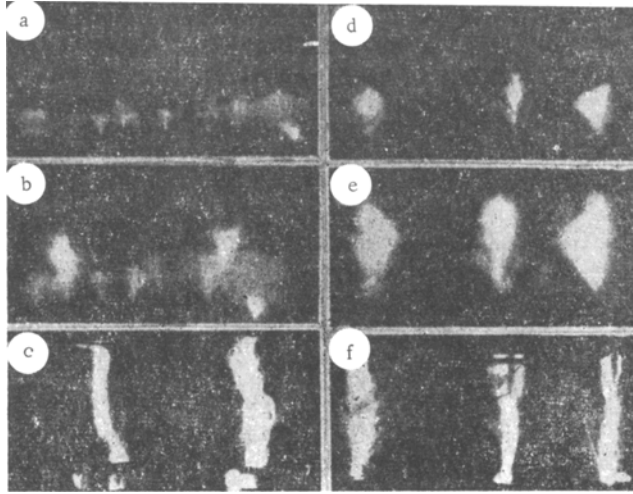


Fig. 3

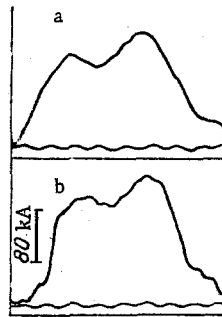


Fig. 4

Three-Channel Trigratron. The discharger consists of two plane electrodes of diameter 20 cm and a radius of curvature of 6 mm, in one of which there are three keep-alive electrodes traced symmetrically on a diameter of 12.5 cm. Each electrode is in the form of a hemisphere 6 cm in diameter (with a wall thickness of 0.4 cm), protruding 3 cm over the common surface. A control electrode 0.5 cm in diameter is placed in an opening 1.4 cm in diameter in the hemisphere. In this construction of the discharger the self-breakdown voltage is 0.9 MV and 1.0 MV for interelectrode distances of 5 and 6 cm, respectively. Taking the data given in [7] into account, the amplitude of the trigger pulse can be taken as +160 kV. In this case the rate of variation of the potential on the trigger electrodes is 10 kV/nsec. The trigger pulse was applied simultaneously to all the control electrodes 0.55 μ sec from the beginning of the charging of the shaping line.

Figure 5 shows the delay time of discharger triggering as a function of the amplitude of the voltage for interelectrode spacings of 5 cm and 6 cm (curves 1 and 2, respectively). Comparing them we see that for the same voltages the time t_d decreases on average by 25-30% when the interelectrode distance is changed by 1 cm, i.e., it increases rapidly as the overvoltage across the main gap of the discharger is reduced. An increase in d (a reduction in the overvoltage) leads to an increase in σ_0 also: for $d=5$ cm, $\sigma_0=8$ nsec and for $d=6$ cm, $\sigma_0=10$ nsec. The more pronounced dependence of t_d on the overvoltage for a trigatron compared with a three-electrode discharger is due to the greater nonuniformity of the field produced by the keep-alive electrode in the trigatron.

The discharger triggers fairly reliably in the range $(0.6-0.95)U_t$. However, satisfactory switching characteristics are only obtained for $U=(0.8-0.95)U_t$, when switching occurs over three channels with a probability of 0.92 (Fig. 3e, the illumination was recorded with an electron-optical converter 170 nsec after applying the triggering pulse to the control electrode). It follows from the pictures obtained from the electron-optical converter and the static photographs that all the channels which are developed at the start of switching (i.e., at the instant when the gap covers at least one channel) at a distance of $\sim 0.6d$ participate in the transmission of the current. The current in these channels at the instant when the switching is completed is $\sim 5-10\%$ of the current in the main channel. In those channels whose length at the start of switching was $0.8d$ or more, the current is $\sim 80\%$ of the current in the channel first connected to the gap [the current in each channel was estimated using the method described in [8], based on the fact that the total output of light (determined from the illumination of the

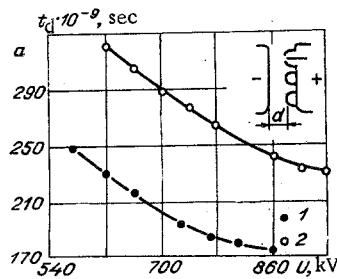


Fig. 5

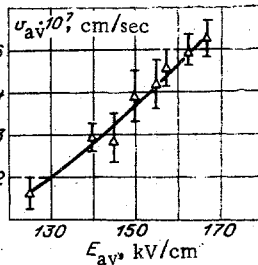


Fig. 6

photograph) is proportional to the energy dissipated in the channel (or the current flowing in the channel), for a constant pulse length]. For optimum values of the charging voltage of $(0.8-0.95)U_t$, the current pulse rise time under three-channel switching conditions is ~ 16 nsec ($I=160$ kA). Thanks to the current distribution over the individual channels (50-55 kA per channel) the erosion of the electrodes is reduced considerably, which ensures more than a thousandfold operation of the discharger without any appreciable deterioration in the switching characteristics.

Using the electron-optical converter, we determined the average velocity v_{av} of increase of the discharge channels at different parts of the interelectrode gap. When several discharge channels are fired simultaneously they all propagate with the same velocity, continuously increasing as they extend into the gap. In the section $(0.1-0.3)d$ the average velocity of increase of the channels is $(0.8-3) \cdot 10^7$ cm/sec. This part is distinguished by the strict directionality of the channels and their only slight branching. In the following section of the path $(0.3-0.7)d$ branching of the channels is observed and a distribution with respect to their rate of increase (Fig. 3d, $U=800$ kV, the illumination was recorded using an electron-optical converter 120 nsec after applying the triggering pulse to the control electrode). A preferential development with a velocity of $(3-5) \cdot 10^7$ cm/sec occurs in those channels which propagate over the shortest path. Over the remaining part of the interelectrode gap v_{av} increases up to $(5-8) \cdot 10^7$ cm/sec. The data given here was obtained for $d=5-6$ cm and an average field strength $E_{av} \approx 160$ kV/cm.

We also measured the average rate of increase of the discharge channels for different field strengths for the same value of $d=5$ cm; Fig. 6 shows the relation between v_{av} and E_{av} , which can be represented in the form of the empirical equation

$$v_{av} = 110E_{av}^{2.6}$$

(v_{av} is in cm/sec, and E_{av} is in kV/cm).

The results show that in switches with a more-uniform field one can produce better conditions which ensure a high rate of development of the discharge processes, and consequently, the range of triggering of the discharger can be broadened with a minimum change in the value of t_d and σ_0 . This can be achieved to a certain extent in a trigatron with a ring keep-alive electrode.

A "Ring" Trigatron. The main electrodes in the discharger ensure that a close to uniform field is obtained. The cathode (a plane disk of diameter 20 cm and radius of curvature 0.6 cm) is a constructional element in the shaping line. The main (anode) and controlling electrodes are connected to the end surface of the transmission line. The main electrode consists of a body made in the form of a hollow disk (wall thickness 0.8 cm) with an internal diameter of 13 cm and an external diameter of 20 cm (radius of curvature 3 cm), and an internal disk 11 cm in diameter, placed at the same level as the surface of the body. The control electrode, made in the form of a ring with a sharp edge (radius of curvature 0.01 cm) of diameter 12 cm, is fastened to

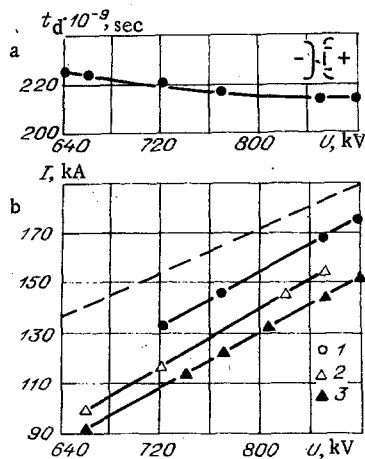


Fig. 7

polyethylene insulators in the internal cavity between the body and the inner disk and protrudes over the surface of the main electrode by 0.2 cm. Hence, between the control and main electrodes there are two gaps of width 0.5 cm. The distance between the main electrodes is 5 cm. This discharger construction enables one, firstly, to obtain multichannel switching with a high triggering stability, and secondly, enables one to increase the number of connections of the discharger due to the extended edge of the control electrode.

As is seen from Fig. 7, unlike the three-channel trigatron (see Fig. 5), in the "ring" trigatron ($d = 5$ cm) t_d depends to a much lesser extent on U , which indicates the high efficiency with which the discharge is initiated by the "intensification of the field" in switches with this kind of electrode geometry. Thus, in the range $(0.75-0.95)U_t$ ($U_t = 950$ kV) the variation in t_d was 3%, while the switching probability over three or more channels (Fig. 7b, curves 3-1 - the switching over one, two and three channels, respectively) is 0.95 (a triggering pulse of amplitude +160 kV was applied to the control electrode 0.55 μ sec after the beginning of the line charging). In this case, as in the previous dischargers, an increase in the amplitude of the switched current by 10-15% is observed (Fig. 7b, curve 1) compared with the single-channel switching mode 3. The instability in the current amplitude is 3-5%.

The results obtained show that by an appropriate choice of the construction and the triggering mode, one can produce water discharges with nanosecond triggering stability, as a result of which multichannel operation can be achieved, which enables the switching time and the electrode erosion to be reduced (thereby increasing the lifetime of dischargers), and enables the efficiency of the circuit to be increased.

LITERATURE CITED

1. J. C. Martin, in: *Nanosecond Pulse Techniques*, Aldermaston, Berks. (1970).
2. B. M. Koval'chuk and Yu. F. Potalitsyn, "Relativistic electron beam generator switches," in: *The Design and Use of Intense Electron Beam Sources* [in Russian], Novosibirsk, Nauka (1976).
3. V. P. Smirnov, "Production of high-current electron beams," *Prib. Tekh. Eksp.*, No. 2, 7-31 (1977).
4. B. Bernstein and I. Smith, "Aurora - an electron accelerator," *IEEE Trans. Nucl. Sci.*, NS-20, No. 3, 294-300 (1973).
5. G. B. Fraizer, "OWL-II pulsed electron beam generator," *J. Vac. Sci. Technol.*, **12**, No. 6, 1183 (1975).
6. V. S. Babintsev, M. G. Korotkov, V. M. Muratov, and V. Ya. Ushakov, "Equipment for investigating dischargers with water insulation at 1MV," in: *The Design and Use of Intense Electron Beam Sources* [in Russian], Nauka, Novosibirsk (1976).
7. W. J. Uschakov, W. M. Muratov, and M. G. Korotkov, "Triggereinrichtung mit flussigen Dielektrikum für Impulsschaltungen hoher Leistung," in: *Nineteenth Intern Scientific Colloquium*, Ilmenau, **5**, 25-30 (1974).
8. J. C. Martin, in: *Multichannel Gaps*, SSWA (ICM), 703/27, AWRE, Aldermaston (1970).